



# Valorization of Biomass Residues by Biosorption of Microelements in a Closed-Loop Cycle

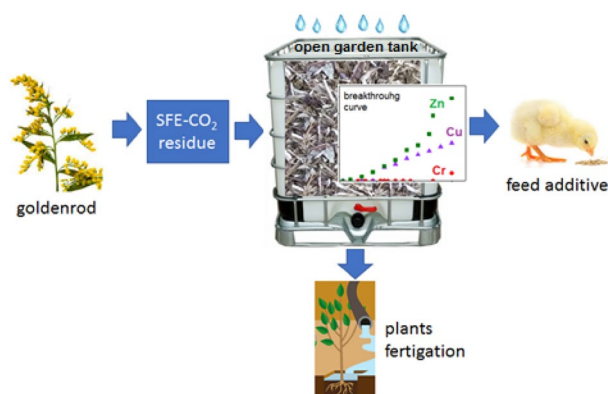
Bartosz Ligas<sup>1</sup> · Jolanta Warchoń<sup>1</sup> · Dawid Skrzypczak<sup>1</sup> · Anna Witek-Krowiak<sup>1</sup> · Katarzyna Chojnacka<sup>1</sup>

Received: 5 July 2021 / Accepted: 12 November 2021 / Published online: 27 November 2021  
© The Author(s) 2021

## Abstract

The concept of the research data presented assumes the valorization of goldenrod residues from supercritical CO<sub>2</sub> extraction following the circular economy principles. The biomass was enriched with microelements (Cr, Zn, Cu) by biosorption from single and multielemental solutions in batch and packed bed reactors. Modeling of biosorption equilibrium supported by instrumental analysis (SEM and FTIR) of material properties was employed to explain the metal ions binding mechanism. The preferential biosorption of Cr(III) over the divalent ions, allows the possibility of valorization of goldenrod residue in a garden-scale biosorption tank acting as a fixed-bed reactor working in an open circulation run and fed with microelements diluted in rainwater. The use of fertigation solution in optimal doses of micronutrients did not show any phytotoxic effect. Using the post-sorptive solution as a source of micronutrients for plants showed significant effects on growth parameters (increased chlorophyll content by 54%) compared to groups fertilized with commercial formulation (13% higher sprout mass). Additionally, fertigation with the post-sorption solution leads to the biofortification of cucumber sprouts. The recycling process results in two products: enriched biomass as a potential feed additive (with Cr(III), Cu(II), and Zn(II)) and a post-sorption solution (with Zn(II) and Cu(II) only) used in the fertigation of plants.

## Graphical Abstract



**Keywords** Biomass valorization · Micronutrients · Feed additives · Fertigation · Waste management

## Statement of Novelty

This work is experimental research that can contribute to achieving sustainability, with respect to its energy use and carbon footprint, by coordinating supercritical CO<sub>2</sub> extraction (SFE-CO<sub>2</sub>) unit owners and small scale farmers. The problem with using SFE-CO<sub>2</sub> solid extraction is

✉ Bartosz Ligas  
bartosz.ligas@pwr.edu.pl

<sup>1</sup> Department of Advanced Material Technologies,  
Faculty of Chemistry, Wrocław University of Science  
and Technology, Smoluchowskiego 25, 50-372 Wrocław,  
Poland

the accumulation of post-processed biomass. Because of its low calorific value, it is not suitable for energy production, so it must be disposed of. Due to the long decomposition time, this operation generates additional costs. To solve that problem we highlighted the idea of enriching the biomass with microelements, by rainwater and salt of trace elements usage. It is a significant advance over past works due to applying the post-treatment solution as a source of micro-nutrients for plant cultivation.

## Introduction

In recent years, the recovery of resources has become one of the main ideas of the sustainable development concept, circular economy, and zero-waste production approach. Major drivers for changing worldwide perception of this problem are projected scarcity of natural resources due to climate change processes, future depletion of non-renewable resources or limitations of their availability, and many socio-economic factors [1].

The European Commission's goal is a reduction by 30% of non-renewable resources used in fertilizer production. This can only be accomplished by waste valorization and the circular economy (CE) approach. A circular economy is a system that is based on the recovery of materials. The European Commission introduced this concept as a response to environmental and social problems [1].

Valorization of plant residue of pharmaceutical, cosmetic, and food origin is a new opportunity for a circular economy enabling biomass used as a food supplement for livestock production [2, 3]. A good example comes from a soybean meal commonly used in livestock farming as a source of assimilable protein. This biomass enriched with Cr, Zn, Fe and Cu ions, added to the laying hens feed, positively affected egg size and increased the transfer of microelements to the yolk fraction [3, 4]. Another waste-turn-into-feed example is cultivated algae *Enteromorpha prolifera* and *Cladophora* sp., used as a hens microelement source. Its application enhanced the size and thickness of eggshells [5, 6]. The biomass of algae enriched with Cu was used in swine breeding, its bioavailability [7]. Feed additives obtained through sorption of Cr, Zn, Cu and Mn ions on alfalfa biomass were used as potential ingredients in feed for hen husbandry [2].

To be used as a feed additive, biomass should meet the appropriate moisture and ash content (2.2%), contain no more than 100 times the standard content of a given substance in a complete meal and be free of faeces, urine, gut contents, treated leather, wood treated with preservatives, package or municipal solid waste and toxic elements [8]. All these requirements are met by plant residues from a supercritical fluid extraction (SFE) process. Thanks to the low

process cost and the lack of necessity for solvents removal, SFE technique fits the trend of green chemistry and political directives limiting the negative impact of industry on the environment [9]. Re-use of the entire remaining post-extraction biomass is the last element required for a waste-free process status acquisition. In this context, valorization of the SFE residues and their usage as a feed additive is in line with the circular economy concept: the use of by-products from one production process as secondary raw material in another.

The by-products of SFE are low-density fibrous materials that are low in nitrogen, soluble carbohydrates, minerals and vitamins, and with varying amounts of lignin and cellulose. The three-dimensional polymer structure of lignocellulose creates the surface area where functional groups suitable for metal binding are localized [10–12] (Volesky and Holan, 1995). For example, methoxyl, hydroxylaliphatic, phenolic, hydroxyl, and carboxyl groups were identified in the polysaccharide cell wall of aster group plants. Phenolic groups are present on the lignocellulose matrix of black locust, while amide and amine groups in the case of ginger [13]. Thus, the presence of lignin and cellulose and types and amounts of functional groups involved are factors enabling biomass enrichment with microelements [14]. Moreover, organoleptic properties of biomass such as taste and smell or the content of medical substances (e.g., flavonoids, saponins) are also under great importance for livestock farming.

European goldenrod (*Solidago virgaurea*) is a perennial flower from the aster family, occurring originally in Europe, central Asia and North America. Beekeepers mainly cultivate this plant because of the positive effect on the taste, colour and health properties of honey [15]. Also, the pharmaceutical industry takes advantage of *Solidago virgaurea* extracts, which contain from 0.5 to 1.5% of flavonoids and other compounds from anthocyanin groups such as saponins and caffeic acid esters. The inclusion of 7.85% hemicellulose, 52.78% lignin and cellulose (with at least 28% of lignin content) [16], acts as a physical barrier impeding the microbial breakdown of goldenrod residue. Such composition extends its fermentation and creates a problem with its storage. So far, the SFE residue of goldenrod is not recycled or used in an alternative way.

This work aims to valorize locally available large quantities of the European goldenrod residues from SFE process and their valorization as a feed supplement enriched with microelements. Chromium (Cr), zinc (Zn) and copper (Cu) were selected as model trace elements in this study due to their dual function in maintaining proper body function of animals and in reducing the negative effect on the heat stress [17, 18]. For example, in the case of laying hens, supplementation with chromium and zinc has been shown to increase the digestibility of nutrients, alleviate effects caused by low ambient temperature [19], and decrease eggshell cracking [20]. Subject to the above, the biosorption of chromium (Cr),

zinc (Zn) and copper (Cu) ions was performed in batch mode for one- and two-component solutions to determine the sorption capacity and goldenrod residues affinity for the tested microelements. The instrumental analysis of biomass before and after metal ions uptake was used for sorbent characterization and the identification of functional groups participating in metal ions binding. Analytical methods were used for quantitative analysis of the carboxyl and hydroxyl groups in the lignocellulose matrix. The mechanism of the metal ions uptake was further supported by modeling of sorption equilibrium.

Moreover, to enrich biomass in a waste-free process, post-biosorption metal solutions were used for the biofortification of cucumber sprouts. It is worth mentioning that both copper and zinc are crucial micronutrients of plant enzymatic, metabolic, and photosynthesis reactions [21, 22]. In opposite, chromium has a well-known phytotoxicity effect for plants, disordering plant germination, root and stem growth, and leaf development [23]. Thus, because of the possible usage of outlet liquid for plant fertigation, an enrichment of biomass with microelements was carried out in a fixed-bed column with identification of the breakthrough time of Cr(III).

## Methodology

### Materials

The biomass of plant residues was obtained as a by-product of the supercritical CO<sub>2</sub> extraction process conducted in the New Chemical Synthesis Institute (Puławy, Poland). As received, post-extraction residues were milled by knife mill (Retsch; grindomix gm300) and sieved to obtain fractions in the range from 0.42 to 0.62 mm.

All chemicals Cu(NO<sub>3</sub>)<sub>2</sub>·3H<sub>2</sub>O (99.0%; Sigma Aldrich; Germany); Zn(NO<sub>3</sub>)<sub>2</sub>·6H<sub>2</sub>O (99.0%; Avantor; Poland); Cr(NO<sub>3</sub>)<sub>3</sub>·9H<sub>2</sub>O (99.0%; Sigma Aldrich; Germany); HNO<sub>3</sub> (69%; Suprapur; Germany) used in this research were of analytical grade. Ultra-pure water (< 0.1 μS/cm, MILLI-Q® HX 7000 SD) was used to prepare the stock solution of metal salts. The initial metal concentrations in single systems were 0–5.9; 0–4.6; 0–4.7 mmol/L for Cr, Zn, Cu, respectively. In each solution, the highest metal ion concentration was equal to 300 mg/L. The initial pH values of single solutions were adjusted to 3.0, 5.6, 4.2 for Cr, Zn, and Cu, respectively. In three binary systems: Cr–Cu, Cu–Zn and Zn–Cr, the initial concentration of both metal ions varied between 0 and 6.0 mmol/L to maintain the constant molar ratio: 1:1:1.

### Characterization of Goldenrod Mass

FT-IR spectroscopy was used to identify the chemical groups present on the biosorbent surface. The infrared

spectra of the biosorbent were recorded in the region of 4000–500 cm<sup>-1</sup> using a Vertex 70v spectrometer (Bruker). The scanning electron microscope (SEM) images were recorded for surface morphology of both “as received” and metal-enriched biomasses at an acceleration voltage of 10 kV (Microscope SEM/Ga-FIB FEI Helios NanoLab™ 600i). The microscope equipped with X-ray spectrometer (EDX) with Silicon Drift Detector was used to confirm the adsorption of metal ions by sorbent. To identify the electrical charge density (pH<sub>pzc</sub>), first, the buffer solution of 0.1 mol/L NaNO<sub>3</sub> was used to adjust pH to a given value by the addition of HNO<sub>3</sub> or NaOH. Then each solution was gently stirred for 30 min with 0.2 g of biomass. The pH<sub>pzc</sub> was determined by Elemetron PCP-401 pH-meter. The content of carboxylic groups in the biomass was identified following [24]. Weighted mass (0.2 g) of biomass was shaken with 10 mL of 0.1 N NaOH and 10 mL of acetone for 2 h. After that, the solution was titrated with 0.1 N with a standard solution of HCl against phenolphthalein. A blank test was performed simultaneously. The number of carboxylic groups in the sample was calculated from the difference in HCl volumes used for the analyzed sample and the blank test. The content of carboxylic groups was calculated from the formula:

$$L_{COOH} = 0.0001(V_{NaOH} - V_{HCl}) \cdot m \quad (1)$$

where  $V$  (mL) is the volume of solution, and  $m$  (g) is the dry mass of biomass. The content of hydroxyl groups in the biomass was identified in accordance with the EU quality standard (PN-EN ISO 2554:2001).

### Sorption Experiments

Adsorption isotherms were obtained by batch sorption experiments. The samples of goldenrod biomass (0.2 g) were gently mixed with 40 mL solution of single or binary component metal salts in a thermostatic shaker (3033, GFL) at 22 °C with 30 rpm. After stirring for 8 h, the suspension was separated from biomass by syringe filters (45 μm cellulose acetate membrane, Millipore), acidified by the addition of conc. HNO<sub>3</sub> (1.0 mL/L), and analyses for their metal content by the inductively coupled plasma optical atomic emission spectrometer (ICP-OES, Varian Vista MPX). Cr was analyzed at a wavelength of 267,716 nm, Cu of 327,395 nm, and Zn of 206,2 nm. The amount of metal adsorbed per unit mass of adsorbent  $q_e$  (mmol/g) was calculated from the equation:

$$q_e = \frac{(C_0 - C_e)}{2} V \quad (2)$$

where  $C_0$  (mmol/L) and  $C_e$  (mmol/L) are the initial and the equilibrium ion concentrations, respectively.

## Modelling of Biosorption Equilibrium

The following empirical models (Eqs. 3, 4, 5) were used to evaluate the metal sorption mechanism in a single-component system:

The Langmuir model (L), which assumes homogenous sorption on the finite number of active sites with equal adsorption energy [25]:

$$q_e = \frac{q_m K_L C_e}{1 + K_L C_e} \quad (3)$$

where  $K_L$  (L/mmol) is the Langmuir constant associated with sorption free energy and sorbent-metal ion affinity,  $q_m$  (mmol/g) is the maximum sorption uptake.

The Freundlich (F) model deals with the heterogeneity of the surface of sorbent towards sorbed molecule [26]:

$$q_e = K_F C_e^{1/n_F} \quad (4)$$

where  $K_F$  signifies sorption capacity per unit concentration (mg/g)/(mg/L),  $1/n_F$  provides information of active sites; the lesser value of  $1/n_F$  indicates the occurrence of heterogeneous sites and the physical sorption mechanism [27].

The Langmuir–Freundlich (L–F) model is a hybrid model that results from the combination of the previous models to circumvent the limitations of both [28]:

$$q_e = \frac{q_m (K_{L-F} C_e)^{n_{L-F}}}{(K_{L-F} C_e)^{n_{L-F}} + 1} \quad (5)$$

where  $K_{L-F}$  (L/mmol) is the Langmuir–Freundlich constant,  $n_{L-F}$  represents the energetic surface heterogeneity. The model's parameters were estimated with the aid of the non-linear regression using Maple software by minimizing the Sum of the Squares of the Errors (ERRSQ):

$$\sum_{i=1}^p (q_{e,\text{exp}} - q_{e,\text{mod}})_i^2 \quad (6)$$

where  $p$  is the number of experimental points,  $q_{e,\text{exp}}$  and  $q_{e,\text{mod}}$  are experimental and the modeling equilibrium concentrations in solid phase, respectively. The fit between experimental and calculated data for all models was evaluated using Fisher's Test (FT), standard deviation ( $\sigma$ ), and mean error (ME) [29].

## Fixed Bed Column Study

The fixed bed experiment was conducted in an open unit run that the main element was a 16 mm (I.D.) glass column of 20 cm height (GE XK 16). The column was packed with a bed (the equivalent of 3 g dry material; 10 cm height). The trinary metal solutions of Cr:Cu:Zn, with an equal

concentration of each metal ion ( $C_{in} = 0.1$  mmol/L of each), were fed to the column by a peristaltic pump (Peristaltic pump Lab 2015; Gkisker) at the gravitational with flow rate 9.0 mL/min. Specimens of eluate were captured from the bottom of the column at specific time intervals and analyzed for metal content by the ICP-OES. The feeding of the column was continued up to 5 h. The experiment was repeated three times.

## Germination Test

Preliminary functional properties of the fertigation solution were performed in germination tests. The experiments were conducted for 10 days at 25 °C and under uniform illumination of 2400 lx (16 h-day, 8 h-night). Cucumber (*Cornichon de Paris*) was selected as the test plant. Fifty cucumber seeds were placed on Petri dishes with moistened cotton wool (5 g). The light-protected dishes were stratified for 48 h at 4 °C. After this time, the dishes were applied NPK fertilizer (13:13:13) in the amount of 50  $\mu\text{m}$ /dish. The fertigation solution was given to the prepared groups at the doses shown in Table 1. The moisture content of the substrate was continuously monitored during germination [30]. After 10 days, the sprouts were analyzed for growth parameters as well as chlorophyll and trace element content. The concentration of the component in the substrate. Statistical analysis was performed using Statistica software (Statsoft, Australia; Tukey's test). The Transfer Factor (TF) was determined using the equation:

$$TF = \frac{C_{\text{plant}}}{C_{\text{substrate}}} \cdot 100 \quad (7)$$

where  $TF$  is considered as transfer factor (%);  $C_{\text{plant}}$  represents the content of the component in the dry weight of the sprout (mg/kg) and  $C_{\text{substrate}}$  provides information about the content of the component in the substrate (mg/kg);

## Results and Discussion

### Biomass Analysis

The scanning electron micrograph revealed the surface texture and morphology of biosorbent (Fig. 1). Sieve tubes of stalk fragments (Fig. 1A, top right corner), leaf structures (left part of the center) and fragments of ligneous plants (right bottom) confirm plant origin and the heterogeneity of the tested sample. The measured diameter of perforations (Fig. 1B) found on the biomass surface (5.05–16.5  $\mu\text{m}$ ) is, on average, ten times larger than the estimated dimensions of xylem and phloem tissue structures [31]. This phenomenon results from the SFE processing of the biomass when

**Table 1** Plan for in vivo testing on plants

Preparation		Fertigation solution	
Plant		Cucumber ( <i>Cornichon de Paris</i> )	
Time		10 days	
Number of seeds per dish		50	
Reference fertilizer		NPK fertilizer (13:13:13) with micronutrients ( <i>YARA HYDROCOTE TM</i> controlled-release fertilizer)	
Dose of NPK (13:13:13) per seed ( $\mu\text{g}$ )		50	
Repetitions		3	
Dose of micronutrients per dish	Dose	Cu	Zn
	%	$\mu\text{g}$	$\mu\text{g}$
	20	40	200
	50	100	500
	100	200	1000
	200	400	1500
	300	600	3000

micro-tissue damage occurs [32]. The high diameter of the biomass' perforations, in comparison to the hydrated ionic radius ( $\text{Cu } 4,19 \text{ \AA} < \text{Zn } 4,30 \text{ \AA} < \text{Cr } 4,61 \text{ \AA}$ ), excludes inner diffusion resistances during ions biosorption [33].

The energy dispersive (EDS) spectra of the goldenrod residue before and after the adsorption of Zn (II), Cu(II), and Cr(III) are shown in Fig. 2. The biomass consisted mainly of C and O. The C:O ratio 1.8:1 is lower than in pure lignin structure (2.16:1) [34]. High surface's C and O content may correlate with the C–C, C–OH, O=C–O, HO–C, O=C, and –OOC–, groups. After metal loading, the EDS analysis of biosorbent identifies the clear peaks of Cr(III), Cu(II), and Zn(II) at 5.6, 8.0, and 8.6 keV, respectively. The obtained percentage by weight of the metals follows the order:  $\text{Cr} > \text{Cu} > \text{Zn}$ . The surface mapping of the received biosorbent in Fig. 3 reveals the presence of Zn and Cu and the lack of Cr on the surface, which is in line with the elemental composition determined by Izydorczyk et al. (2020). In opposite to Cr(III), both Cu(II) and Zn(II) are essential redox-active metals that participate in many physiological processes in plant materials [35].

The FTIR spectra of goldenrod biomass before and after metal ions sorption are shown in Fig. 4. The presence of broad absorbance in the range of  $3500$  to  $3300 \text{ cm}^{-1}$  represents carbohydrates [36]. The identified peak at  $3435 \text{ cm}^{-1}$  is assigned to the carboxylic stretching band or alcohol groups [37]. The peak at  $2926 \text{ cm}^{-1}$  may be associated with O–H stretching of the carboxylic acid in the cell wall of the biomass. This peak is followed by the stretching at  $2852$  visible after metal sorption, corresponding to the aliphatic C–H group of organic chains of the cellulose [38]. The band between  $1700$  and  $1750 \text{ cm}^{-1}$  attributes to C=O

stretching vibration indicates the presence of a variety of functional groups: carboxylic, ester, quinone, conjugated aldehyde, conjugated ketone,  $\alpha\beta$  unsaturated ester and aliphatic ketone [39]. The peak at  $1734 \text{ cm}^{-1}$  corresponds to the content of sesquiterpene lactones remaining in plant tissue after extraction [40]. The bands that appeared in the range of  $1740$ – $1050 \text{ cm}^{-1}$  are related to polysaccharides with different structures and configurations. The registered band about of  $1638 \text{ cm}^{-1}$ , relates to asymmetric and symmetric C=O bands of carboxylic, ester or aldehyde vibrations [41, 42]. Their shift after metal ion sorption indicates a degree of carboxyl bonding. The pattern of aromatic vibration near  $1600 \text{ cm}^{-1}$  and  $1500 \text{ cm}^{-1}$ , along with the peaks near  $1200 \text{ cm}^{-1}$  is attributed to aryl–O stretching vibration and confirms the presence of lignin. The visible and narrow peak at  $1384 \text{ cm}^{-1}$  appeared only after metal ions sorption and may be attributed to symmetric stretching of –COO– [43]. Two flattened peaks at  $1320$  and  $1254 \text{ cm}^{-1}$  are assigned to  $\text{CH}_2$  symmetric and C–H bending caused by the stretching of syringyl and guaiacyl rings of lignin and lignocellulose [44]. These bands can also correspond to the C=O stretching of ester and carboxylate groups [45]. After metal ions sorption, their position and intensity do not remain the same, further confirming the interaction of metal ions with carboxylic groups. The peak at  $1052 \text{ cm}^{-1}$  may indicate by the presence of C–O vibrations caused by a large amount of polysaccharides or polysaccharide-like substances [46]. The observed vibrations in the  $800$ – $600$  range relate to the presence of C–C bonds being the core of the biomass.

The presence of carboxyl and hydroxyl groups was further confirmed by chemical analysis. The total number of identified carboxylic groups was  $1.33 \text{ mmol/g}$ , while



**Fig. 1** SEM–EDS micrograph of **A** biomass and loaded with **B** Zn, **C** Cu, **D** Cr

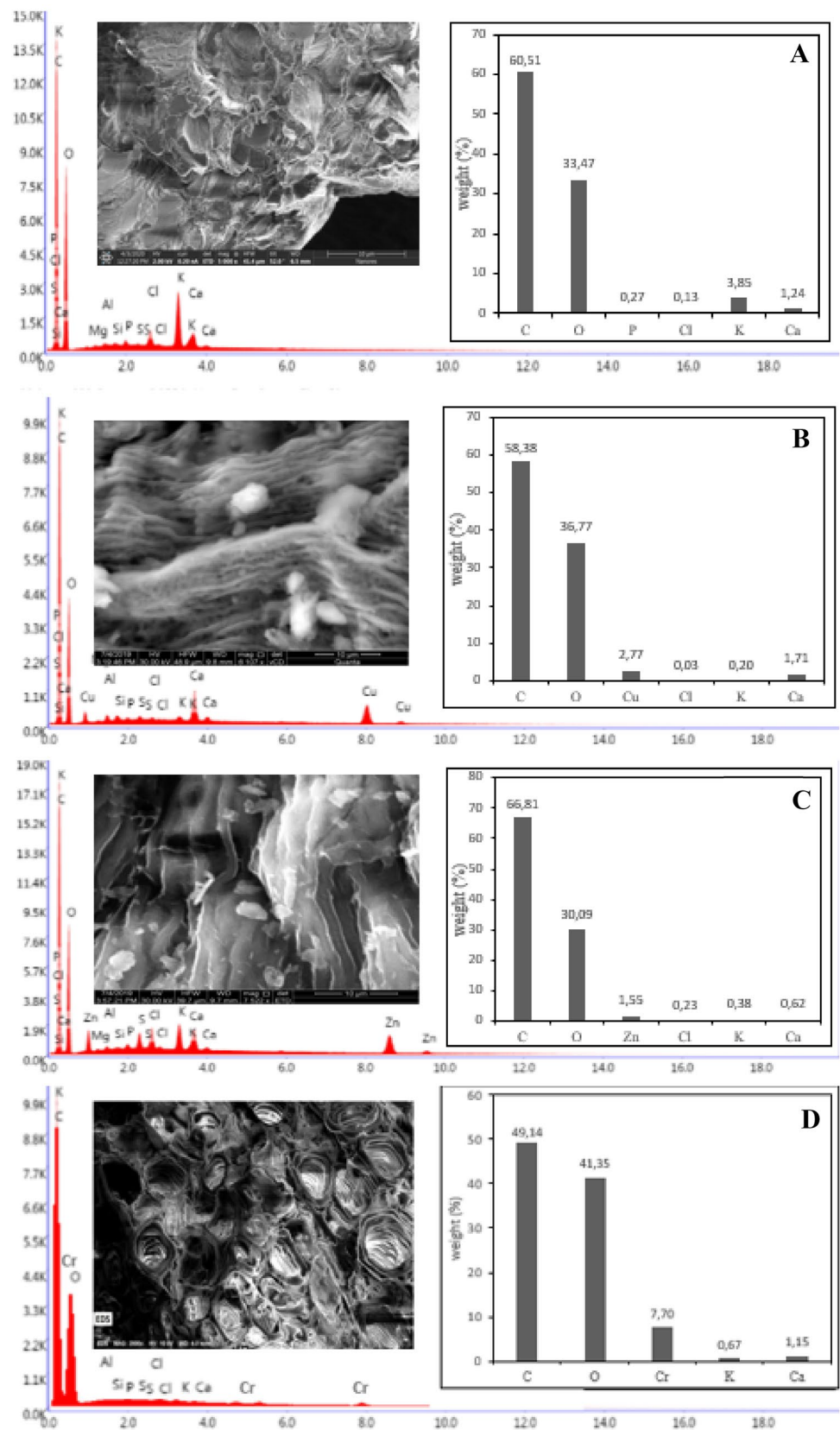


**Fig. 2** Scanning electron micrography of goldenrod residues

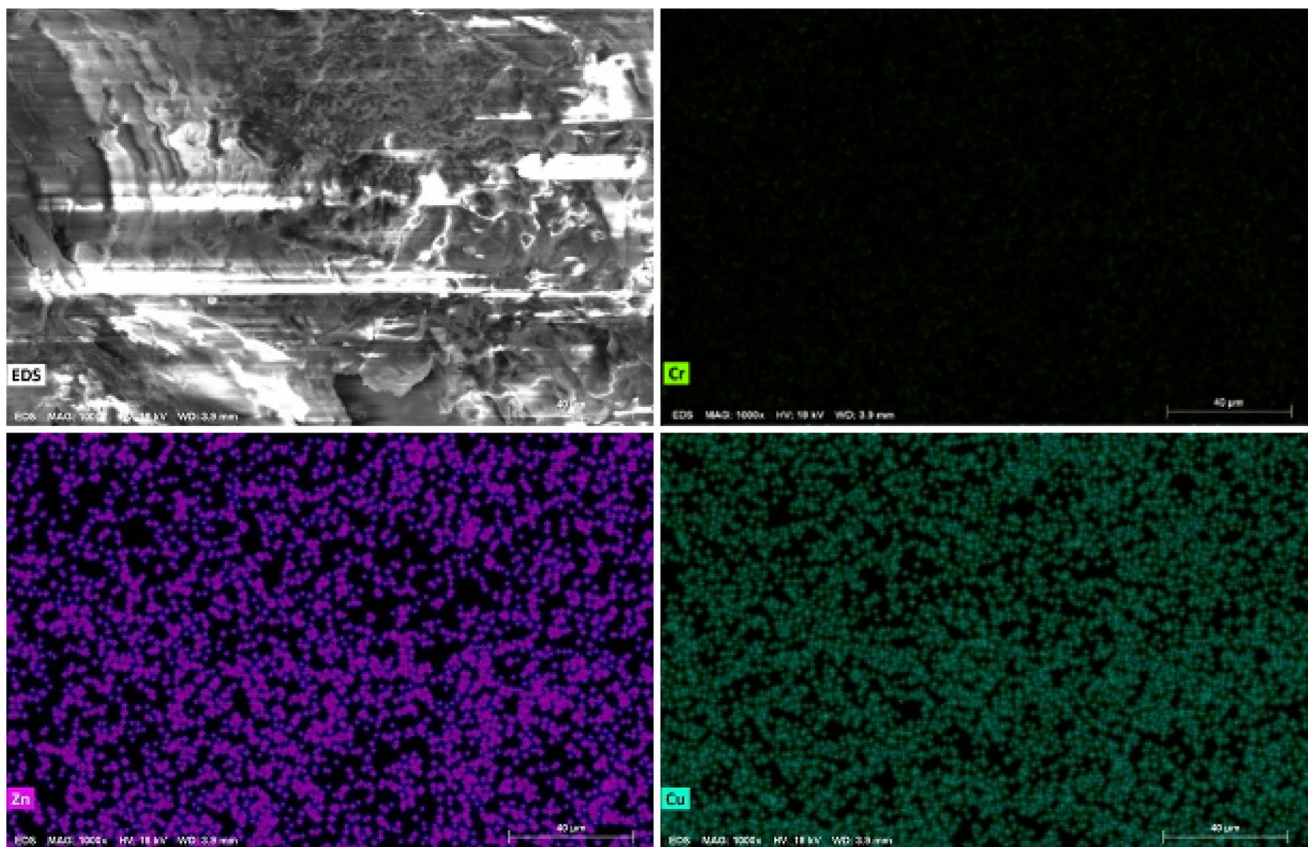
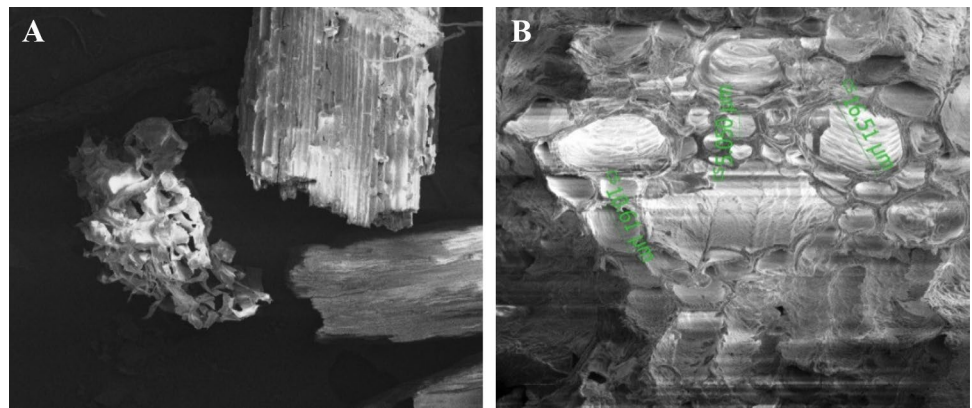
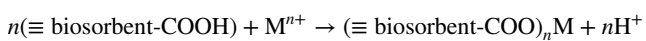


**Fig. 3** Elemental dot maps of the goldenrod residue

the hydroxyl one was 0.83 mmol/g. According to the above, the main mechanism of metal ions binding can be expressed as:



where  $M^{n+} = Zn^{2+}$ ,  $Cu^{2+}$ , and  $Cr^{3+}$  ions.

The formation of M–O bonds between metal ions and the acid functional groups of lignocellulosic sorbents was confirmed by other authors with XPS analysis [47].

Nevertheless, metal ions binding via bridging complexation, ion exchange or chelation cannot be excluded.

### Biosorption Isotherms

The experimental data depicted in Fig. 5 represent the equilibrium distribution of the metal ions between the goldenrod biomass and the residual metal concentration in the liquid phase. The data exhibit nonlinearity in the uptake of every metal. As can be seen, the experimental isotherms for all

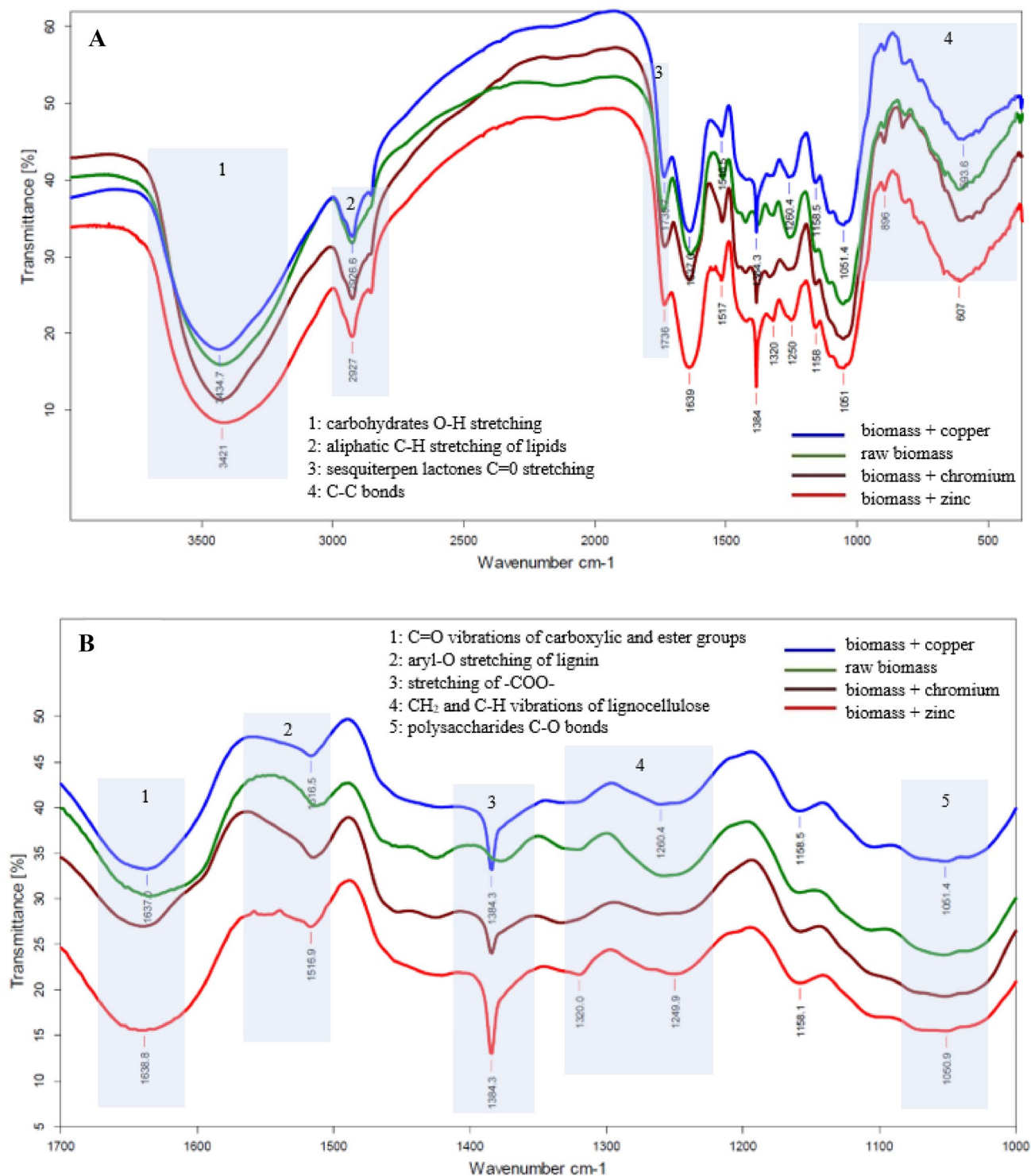


**Fig. 4** FTIR spectra of goldenrod residues before and after metal sorption (**A** whole spectrum, **B** 1700–1000  $\text{cm}^{-1}$  range magnification)

metal ions overlapped each other without clear identification of biomass affinity for a given metal ion. None of the isotherms reaches the sorption plateau. The values of the maximum sorption capacity obtained are close to each other.

The equilibrium  $\text{pH}_{\text{eq}}$  values changed along with the concentration of the components and varied between  $\text{pH}$  5.3–4.6 for Zn;  $\text{pH}$  4.4–3.0 for Cr; and 5.5–3.9 for Cu. The measured isoelectric point (pI) of goldenrod is about 5.1. Thus, under



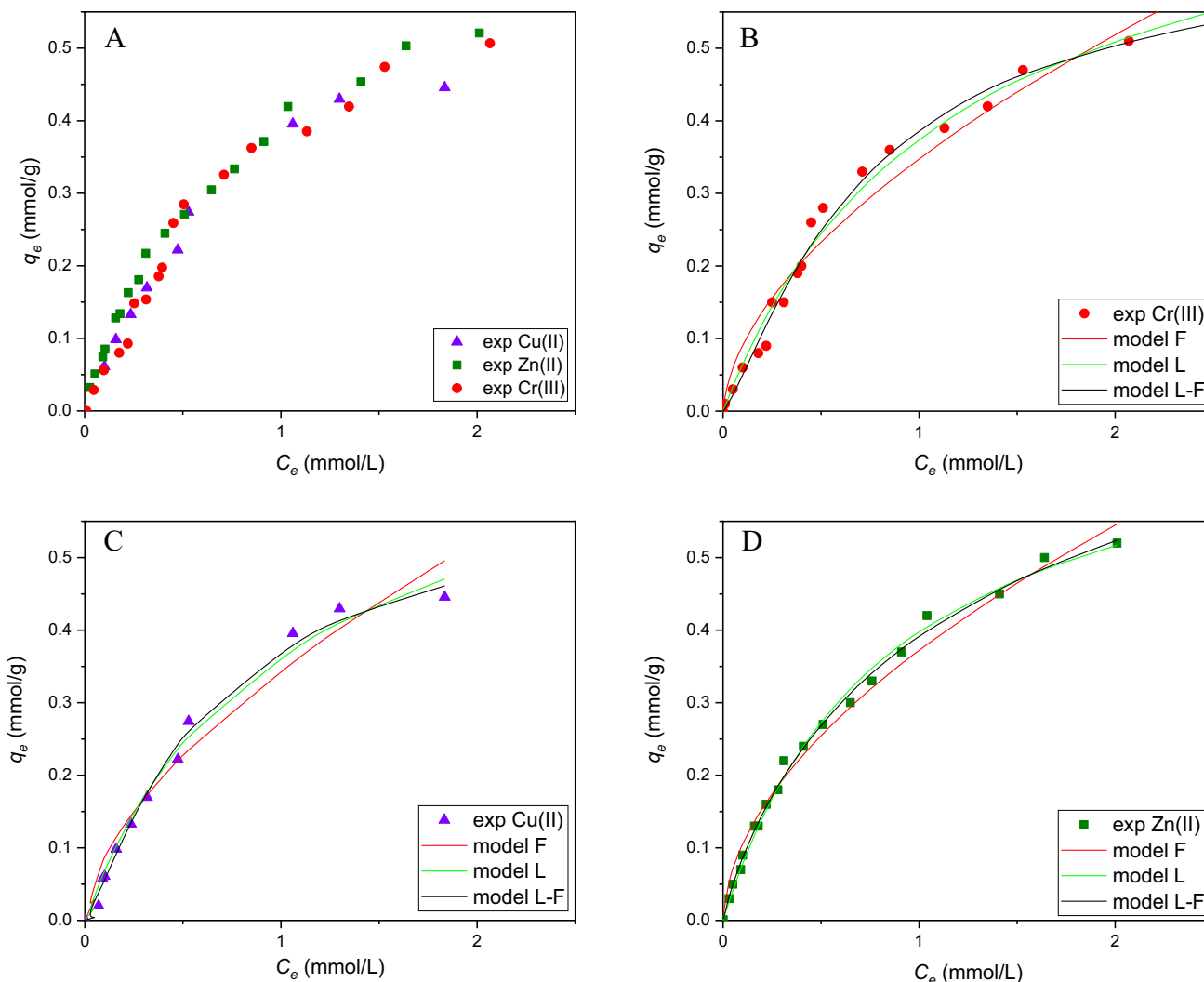


**Fig. 5** Comparison between equilibrium models and experimental data obtained for single systems

the obtained  $pH_{eq}$  ranges, most of the carboxylic acid groups were ionized ( $pH_{eq} > pH_{pzc}$ ), causing a strong electrostatic attraction between the sorbent surface (negatively charged) and the heavy metal ions [48].

The modeling of biosorption equilibrium was done by using three empirical equations. The values of fitting parameters are depicted in Table 1. Among the applied models, the three-parameter Langmuir–Freundlich model best fit the experimental data, as can be seen from the value of statistical tests. This model closely overlapped the Langmuir one. The maximum sorption capacities estimated from both models were higher than the obtained experimentally ( $q_{m,exp}$ ). The values of parameter  $n_{L-F} \neq 1$  provide the multiple and energetically heterogeneous biosorption.

The comparison of  $q_m$  obtained for single and binary solutions (Fig. 6A) identifies that the efficiency of metal ions biosorption from binary solutions is lower than from

a single one. This is the case when metal ions compete for the same active sites and share them [47]. The most remarkable is the magnitude of this effect which differs for a given ionic pair. The observed reduction of Cr(III) biosorption in the presence of Zn(II) and Cu(II) is lowered by about 20% and 40%, respectively, in comparison to the single Cr(III) solution. In comparison, the reduction of Zn(II) and Cu(II) biosorption in the presence of Cr(III) is lowered by about 10 times for single solutions. Furthermore, the shape of the binary Cr–Cu and Zn–Cr isotherms (Fig. 6C, D) reveals that the equilibrium concentration of Cr(III) constantly increases in the whole equilibrium range. In turn, the equilibrium concentration of Zn(II) and Cu(II) increases only at low concentrations values, decreasing then sharply. In the case of the Cu–Zn system, a clear co-sorption is seen from overlapping both isotherms at a lower concentration range. Then, the antagonistic effects of Cu(II) over Zn(II) are observed.

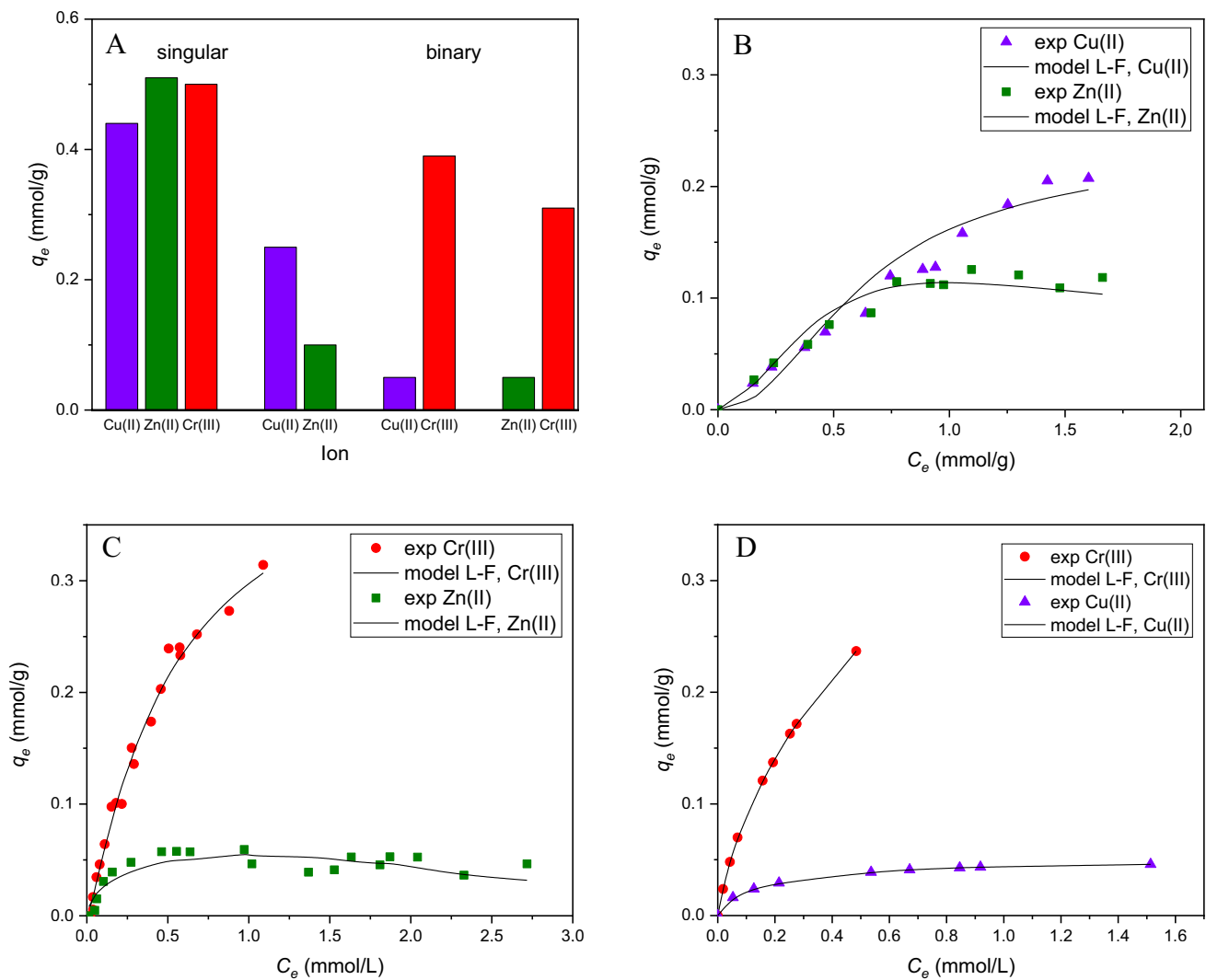


**Fig. 6** Comparison between the Langmuir–Freundlich model and experimental data obtained for binary systems

Cu(II), as a more favorable ion, exchanged Zn(II) in active sites, decreasing its sorption. As stems from the binary isotherms, the affinity of the goldenrod residues for tested metal ions follows the order: Cr(III) > Cu(II) > Zn(II).

The linear extensions of the L–F model derived by adding one more concentration term were used for modeling of antagonistic sorption of heavy metal ions [47]:

$$q_{e1} = \frac{q_{m1}(K_{L-F1}C_{e1})^{n1}}{(K_{L-F1}C_{e1})^{n1} + (K_{L-F2}C_{e2})^{n2} + 1}, q_{e2} = \frac{q_{m2}(K_{L-F2}C_{e2})^{n2}}{(K_{L-F1}C_{e1})^{n1} + (K_{L-F2}C_{e2})^{n2} + 1} \quad (8)$$

where subscripts 1 and 2 relate to the given pair of metal ions in a binary system (Cr–Cu, Zn–Cr, Cu–Zn). In the binary equilibrium calculation procedure, the parameter sets obtained for single systems were used as an initial guess to

minimize the ERRSQ objective function across the concentration range studied [49].

The comparison of the experimental and modeling data in Fig. 6B–D demonstrates that the extended Langmuir–Freundlich model fits the binary equilibrium points reasonably well. The model’s parameter values, together with statistical test results, are depicted in Table 2. Apparently, the biosorp-

tion capacity of Cr(III) is higher than that of Cu(II) and Zn(II), showing the higher affinity of goldenrod residue for Cr(III). As it steams from Table 2, Cr(III) follows homogeneous sorption since  $n_{L-F} \approx 1$ . Nevertheless, the estimated

**Table 2** Equilibrium constants for the single biosorption of Zn(II), Cu(II) and Cr(III) ions on goldenrod residues

Metal ion	Model	$q_m$ (mmol/g)	$n_{L-F}$	$K_{L-F}$ (L/g)	$TF$	$\sigma$	ME (%)
Zn	L	0.73	n.e	1.19	215.71	5.77	0.01
	$q_{m,exp}=0.51$	F	n.e	1.83	76.08	50.45	0.02
	(mmol/g)	L-F	0.78	0.86	0.87	287.51	7.50
Cu	L	0.71	n.e	1.04	105.69	31.90	0.02
	$q_{m,exp}=0.46$	F	n.e	0.34	28.24	199.55	0.03
	(mmol/g)	L-F	0.57	1.24	1.63	287.50	7.49
Cr	L	0.80	n.e	0.88	71.46	11.48	0.02
	$q_{m,exp}=0.50$	F	n.e	1.73	24.31	29.58	0.03
	(mmol/g)	L-F	0.64	1.25	1.38	88.40	13.2

**Table 3** The Langmuir–Freundlich constants for the binary biosorption on goldenrod residues

Binary system	$q_{m1}$	$n_{L-F1}$	$q_{m2}$	$n_{L-F2}$	$TF$	$\sigma$
1 2	(mmol/g)		(mmol/g)			
Cr-Cu	1.21	1.01	0.09	0.61	40.39	0.03
Zn-Cr	0.13	0.48	0.85	1.08	44.27	0.83
Cu-Zn	0.26	2.28	0.66	1.66	26.14	0.09

values of  $q_m$  are higher than the experimentally obtained ones (see Tables 2, 3). This results from the fact that modeling calculations were performed only for one molar ratio experimental set (1:1:1) and the obtained isotherms' curves had a grove up tendency.

**Triple-Biosorption Breakthrough Curves**

The envisaged higher affinity of the biomass for Cr(III) than Cu(II) and Zn(II) creates an opportunity to the enrichment of the SFE residue in a close free-waste processing cycle. Thus, the competitive biosorption of Cr(III), Cu(II) and Zn(II) ionic mixture under continuous conditions was evaluated on a laboratory scale. The breakthrough curves depicted in Fig. 7 are expressed in terms of normalized concentration, defined as the ratio of effluent metal concentration to influent metal concentration ( $C/C_{in}$ ), as a time (t) function. As can be observed from the plots grow up, all breakthroughs obtained have a flatter concave shape. The fastest bed saturation was achieved for Zn(II). In the case of this ion,  $C/C_{in} > 1$ , which identified its replacement by competitive ions. The metal ions breakthrough points follow the order: Zn (5 min) > Cu (9 min) > Cr (25 min). The Cr(III) breakthrough point is when the biomass enrichment process should be stopped to prohibit Cr(III) appearance in the liquid outlet. As can be seen from the picture magnification, up to 25 min of liquid flow Cr(III) is sorbed on biomass, while the content of Cu(II) and Zn(II) in the liquid outlet tends to increase. The adsorption loading of metal ions up to 25 min of filtration (magnification on Fig. 7) was obtained by integration of the area under the breakthrough curve, at  $C_{in}$  feeding concentration and  $\bar{V}$  flow rate, by using the following equations:

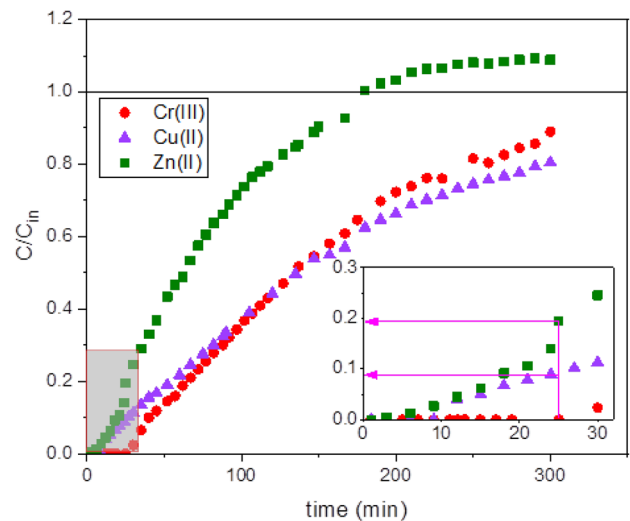


**Fig. 7** Breakthrough curves for triple metal ions biosorption

$$q_t = \frac{\bar{V}}{m_b} \int_{t=0}^{t=25} (C_{in} - C(t))dt \tag{9}$$

$$q_t \approx \frac{\bar{V}}{m_b} \sum_{i=0}^p (C_i - \bar{C}) \cdot (t_{i+1} - t_i) \text{ and } \bar{C} = (C_{i+1} + C_i)/2 \tag{10}$$

where  $t$  (min) is time,  $m_b$  (g) is mass of bed,  $\bar{V}$  is volumetric flow rate (mL/min),  $C_i$  is an effluent concentration (mmol/L) at given  $i$ .

The calculated amount of metal ions sorbed by the biomass in the first 25 min of the process, equals 0.39 mgCr/g

(0.0075 mmol/g), 0.43 mgCu/g (0.0067 mmol/g) and 0.41 mgZn/g (0.0063 mmol). The obtained biomass enriched with microelements can be used as a feed additive, for e.g., chickens. As demonstrated by scientific studies, the chromium content in a food additive positively affected laying eggs efficiency [50] and on chicken growth [51]. Considering the obtained values of  $q_t$  for Cu and Zn, their content did not exceed the UE regulation levels allowed in poultry feed (35 and 250 mg/kg, respectively) [52]. Furthermore, the usage of enriched goldenrod residue as a food additive can enrich poultry feed with cellulose, the main fiber component.

The concentration of Cr, Cu, and Zn in the outlet solution, which was collected over 25 min of filtration, was calculated from the equation:

$$C_t = \frac{\bar{V} \cdot \sum_{i=0}^p \left( \frac{C_{i+1} + C_i}{2} \right) \cdot (t_{i+1} - t_i)}{V_t} \quad (11)$$

where  $V_t$  (mL) is the volume of effluent collected during 25 min of filtration.

The values obtained were as follows: 0 mgCr/L, 0.68 mgCu/L, and 0.80 mgZn/L. The latter two amounts are higher than recommended in commercially available liquid fertilizers for fertigation (0.12 mgCu/L and 0.35 mgZn/L) but lower than recommended for foliar fertilizers (Mikroplus; Intermag). Obviously, for lower concentrations of all metals in column inlet, the binding sides would be occupied slower and more time would be needed to saturate the column bed. However, to delay the breakthrough time of Cr(III) in relation to the divalent ions, it would be more appropriate to reduce its initial concentration in the inlet solution.

The research indicates the potential for biomass enrichment with metal ions in a closed-loop cycle in the fertigation and feed additives industry. For example (Fig. 8), a

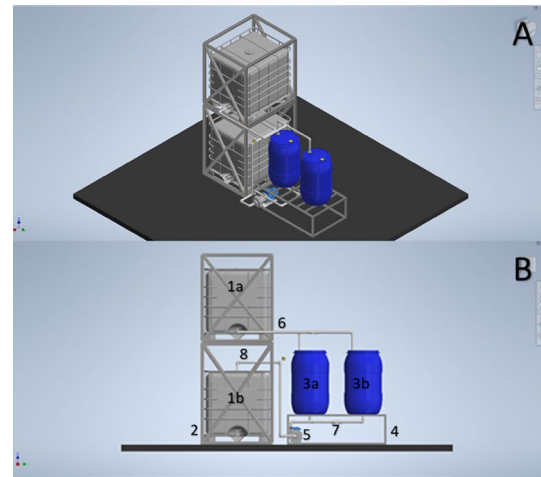


**Fig. 8** Model of a garden-scale biosorption plant (Inventor 2021; Autodesk, USA)

garden-scale biosorption tank can consist of two intermediate bulk containers, placed one on top of the other. The top container would act as a rainwater collector with dissolved salt of microelements. It should have a valve to gravitationally feed the bottom container. The latter would act as a fixed bed reactor filled with any lignocellulose residues. The bottom container should be equipped with two punctured shelves allowing bed packing and preventing biomass floating and with an outlet valve. After filtration, biomass ought to be sun-dried to prevent rotting, while the collected outlet solution, after dilutions, is used for the plants fertigation.

To potentially reduce the construction costs, the selection of the plant components was made based on commercially available components. The model consists of two 1000L Mauzer tanks (1a and 1b) with support system (2), two polypropylene tanks (3a and 3b), a frame supporting

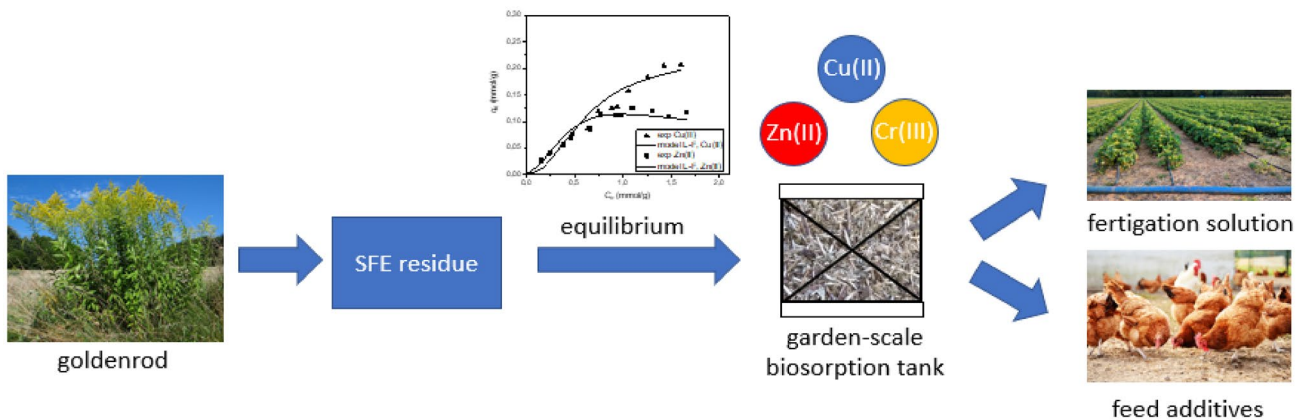


**Fig. 9** Ideological diagram of work



**Table 4** Effect of micronutrient dose on growth parameters of cucumber sprouts (0–unfertilized group, KN—group fertilized with commercial formulation, 20–300 groups fertilized with fertigation solution)

Dose %	Fresh mass g	Chlorophyll mg/m <sup>2</sup>	Stem length cm
0	8.23 ± 0.114 <sup>a,b,c,d,e</sup>	538 ± 52.6 <sup>a,b,c</sup>	1.82 ± 0.324 <sup>a,b,c,d,e</sup>
100 (KN)	10.7 ± 0.164 <sup>a,f,g,h</sup>	507 ± 54.0 <sup>d,e,f,g,h</sup>	2.71 ± 0.372 <sup>a,f,g,h</sup>
20	11.3 ± 0.232 <sup>b,i</sup>	609 ± 34.9 <sup>a,d</sup>	2.68 ± 0.370 <sup>b,l,m,n</sup>
50	11.8 ± 0.216 <sup>c,f,j,k</sup>	598 ± 26.1 <sup>b,e</sup>	3.03 ± 0.322 <sup>c,o,p,r</sup>
100	12.0 ± 0.021 <sup>d,g,l,m</sup>	592 ± 34.8 <sup>f</sup>	3.55 ± 0.323 <sup>d,f,l,o,s,t</sup>
200	10.6 ± 0.427 <sup>e,h,j,l,n</sup>	609 ± 27.5 <sup>c,g</sup>	2.29 ± 0.342 <sup>e,g,m,p,s,u</sup>
300	7.70 ± 0.21 <sup>i,k,m,n</sup>	593 ± 41.7 <sup>h</sup>	1.70 ± 0.267 <sup>h,n,r,t,u</sup>

<sup>a,b,c,...</sup> Statistically significant differences relative to the zero and reference groups—Tukey test ( $p < 0.05$ , vertical comparison)

the tank (4), a centrifugal pump (5) and a set of valves and pipes transporting the fluids (6, 7, 8).

The proposed residue valorization is an energy-free process, using rainwater as a renewable liquid, which would allow achieving circular economy status for the SFE technique (Fig. 9).

### Seeds Germination and Plant Growth

Germination tests were conducted at a laboratory scale to evaluate crop promotion products for phytotoxicity and bioavailability of elements [53]. Germination is a crucial stage of plant growth that is influenced by both internal and external factors. The most important factors of the process include moisture, temperature and light, providing these conditions allows for objective assessment of the effectiveness of formulations [54]. This process causes a number of biochemical changes inside the seed and the accumulation of health-promoting components. Extremely high contributions in the initial stages of growth are micronutrients from the group of Cu, Mn, and Zn, which affect the plant's sustainable development [55].

Analyzed parameters of cucumber sprout growth (stem length, fresh sprout weight, chlorophyll content) are presented in Table 4 and Fig. 10. The highest fresh sprout mass (12.0 g) was achieved in the group fertilized with a dose of 100% of micronutrient demand. The obtained sprout mass was about 13% higher compared to the group fertilized with a commercial product. Groups fertigated with doses above the optimum showed a phytotoxic effect. A similar effect can be observed in the case of stem length, where maximum length was found in a group with an applied dose of 100%. For mass and stem length, statistically significant differences were found between almost all groups. A different effect was observed for chlorophyll content, where statistically significant differences occurred only between the zero and control

groups and the groups fertigated with the solution after the biosorption process. This effect can be correlated with the high zinc content of fertigated sprouts (Table 5). This element plays a significant role in the structure of chloroplasts [56].

The crucial parameter in assessing the bioavailability of nutrient formulations is TF, which describes the content of micronutrients in the plant relative to the amount applied to the substrate [57]. The coefficient decreases with increasing micronutrient dose, which is closely related to the plant's limited demand for selected micronutrients (Table 4) [58]. At the optimum dose, the TF was twice as high as the group fertilized with commercial fertilizer. After biosorption, the components present in the solution are in ionic form, which is the most bioavailable form, significantly affecting their transfer and accumulation in the plant [59]. Statistically significant differences occurred between almost all groups, excluding the control group and selected fertigated groups.

Preliminary evaluation of solution utilization efficiency after the biosorption process confirmed the possibility of waste management for agricultural purposes. It can be concluded that the high bioavailability of components in the ionic form leads to biofortification of cucumber sprouts, which furtherly can result in the cultivation of highly nutritious functional foods [60].

### Summary

The SFE goldenrod residues are lignocellulose materials with a high content of carboxyl and hydroxyl functional groups suitable for metal ions binding. Equilibrium studies for single metal solutions did not identify any preferred sorption of tri or divalent ions. The higher affinity of biomass for Cr(III) has been proved only after the binary equilibrium tests. The obtained sequence of affinity: Cr(III) > Cu(II) > Zn(II) was furtherly confirmed in the fix-bed study. The breakthrough time for Cr(III) was the longest compared to other ions, and the process termination ensured the absence of Cr(III) in the outlet solution. The metal ions content in enriched biomass for Cr, Cu, and Zn was equal: 0.0075, 0.0067 and 0.0063 mmol/g. Due to the presence of microelements and cellulose, the enriched biomass can be applied as a feed additive. The collected filtration solution contained 0.011 mmol Cu/L and 0.012 mmol Zn/L can be used for the plants fertigation. Using the post-sorptive solution as a source of micronutrients for plants showed significant effects on growth parameters compared to groups fertilized with commercial formulation (13% higher sprout mass).

**Fig. 10** Effect of micronutrients dose on stem length (A) and chlorophyll content (B) of cucumber sprouts (0-unfertilized group, KN—group fertilized with commercial formulation, 20–300 groups fertilized with fertigation solution)

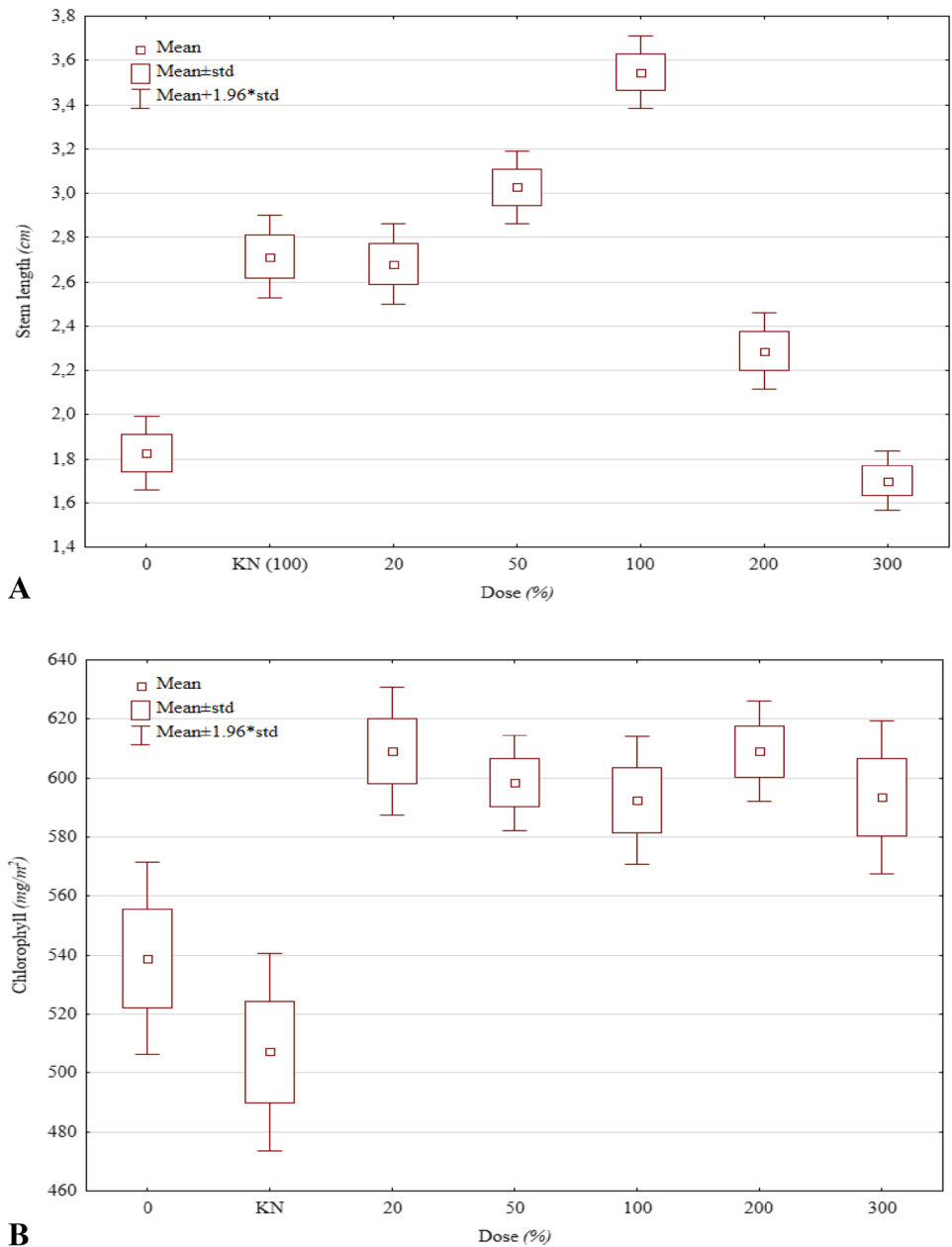


**Table 5** Effect of micronutrient dose on micronutrient content in sprout and Transfer Factor (0-unfertilized group, KN—group fertilized with commercial formulation, groups fertilized with fertigation solution)

Dose	Content		TF	
	mg/kg		%	
%	Cu	Zn	Cu	Zn
0	7.81 ± 0.628 <sup>a,b,c,d,e,f</sup>	44.3 ± 1.93 <sup>a,b,c,d,e,f</sup>	—	—
100 (KN)	31.1 ± 0.469 <sup>a,g,h,i,j</sup>	152 ± 0.61 <sup>a,g,h,i,j</sup>	10.3 ± 0.156 <sup>a,b,c,d</sup>	10.1 ± 0.041 <sup>a,b,c,d</sup>
20	35.2 ± 0.640 <sup>b,k,l,m,n</sup>	173 ± 1.16 <sup>b,k,l,m</sup>	62.7 ± 1.144 <sup>a,e,f,g,h</sup>	61.9 ± 0.413 <sup>a,e,f,g,h</sup>
50	47.2 ± 0.696 <sup>c,g,k,o,p,r</sup>	218 ± 3.54 <sup>c,g,n,o,p</sup>	78.2 ± 1.153 <sup>b,e,i,j,k</sup>	36.1 ± 0.587 <sup>b,e,i,j,k</sup>
100	61.8 ± 2.260 <sup>d,h,l,o,s,t</sup>	288 ± 14.1 <sup>d,h,k,n,r,s</sup>	54.3 ± 1.984 <sup>c,f,i,l,m</sup>	25.2 ± 1.234 <sup>c,f,i,l</sup>
200	133.9 ± 4.331 <sup>e,i,m,p,s</sup>	457 ± 22.3 <sup>e,i,l,o,r</sup>	26.7 ± 0.862 <sup>d,g,j,l,n</sup>	24.3 ± 1.185 <sup>d,g,j,m</sup>
300	133.6 ± 5.384 <sup>f,j,n,r,t</sup>	443 ± 15.0 <sup>f,j,m,p,s</sup>	13.3 ± 0.537 <sup>h,k,m,n</sup>	8.84 ± 0.300 <sup>h,k,l,m</sup>

<sup>a,b,c,...</sup> Statistically significant differences relative to the zero and reference groups—Tukey test (p < 0.05, vertical comparison)

## Conclusions

The enrichment of the SFE residue with microelements with a view of its use as a food additive closes the loop of the goldenrod plant processing cycle. Furthermore, the utilization of post-biosorption metal solutions for fortification of plants makes the enrichment process waste-free. Due to the toxic effect of chromium on plant, the enrichment of biomass with Cr, Cu, and Zn ions should be performed in a fixed-bed column, which enables biosorption termination when Cr appears in column outlet. Due to this, it is possible to obtain two products: enriched in Cr, Cu, and Zn food additive, and fertigation liquid containing Cu and Zn. The closed circuit of microelements classifies the presented technique as environmentally friendly according to European Union standards.

**Acknowledgements** This project is financed in the framework of grant entitled: “Cultivated plants and natural products as a source of biologically active substances assigned to the production of cosmetic and pharmaceutical products as well as diet supplements” (No. BIOSTRATEG2/298205/9/NCBR/2016) attributed by the National Centre for Research and Development.

**Author Contributions** All authors contributed to the study's conception and design. Material preparation, data collection and analysis were performed by BL, and DS. BL wrote the first draft of the manuscript and all authors commented on previous versions of the manuscript. All authors read and approved the final manuscript.

**Funding** This project is financed in the framework of grant entitled: “Cultivated plants and natural products as a source of biologically active substances assigned to the production of cosmetic and pharmaceutical products as well as diet supplements” (no. BIOSTRATEG2/298205/9/NCBR/2016) attributed by the National Centre for Research and Development.

**Data Availability** The data that support the findings of this study are available on request from the corresponding author.

**Code Availability** Not applicable.

## Declarations

**Conflict of interest** The authors declare that they have no known competing financial interests or personal relationships that could have appeared to influence the work reported in this paper.

**Open Access** This article is licensed under a Creative Commons Attribution 4.0 International License, which permits use, sharing, adaptation, distribution and reproduction in any medium or format, as long as you give appropriate credit to the original author(s) and the source, provide a link to the Creative Commons licence, and indicate if changes were made. The images or other third party material in this article are included in the article's Creative Commons licence, unless indicated otherwise in a credit line to the material. If material is not included in the article's Creative Commons licence and your intended use is not permitted by statutory regulation or exceeds the permitted use, you will need to obtain permission directly from the copyright holder. To view a copy of this licence, visit <http://creativecommons.org/licenses/by/4.0/>.

## References

- Ritzén, S., Sandström, G.Ö.: Barriers to the circular economy - integration of perspectives and domains. In: Procedia CIRP (2017)
- Michalak, I., Godlewska, K., Marycz, K.: Biomass enriched with minerals via biosorption process as a potential ingredient of horse feed. *Waste Biomass Valoriz.* **10**, 1–16 (2018). <https://doi.org/10.1007/s12649-018-0351-5>
- Witkowska, Z., Świniarska, M., Korczyński, M., Opaliński, S., Konkol, D., Michalak, I., Saeid, A., Mironiuk, M., Chojnacka, K.: Biofortification of hens' eggs with microelements by innovative bio-based dietary supplement. *J. Anim. Physiol. Anim. Nutr. (Berl)* **103**, 485–492 (2019). <https://doi.org/10.1111/jpn.13027>
- Witkowska, Z., Chojnacka, K., Korczyński, M., Świniarska, M., Saeid, A., Opaliński, S., Dobrzański, Z.: Soybean meal enriched with microelements by biosorption: a new biological feed supplement for laying hens. Part I. Performance and egg traits. *Food Chem.* **151**, 86–92 (2014). <https://doi.org/10.1016/j.foodchem.2013.11.023>
- Saeid, A., Chojnacka, K., Opaliński, S., Korczyński, M.: Biomass of *Spirulina maxima* enriched by biosorption process as a new feed supplement for laying hens. *Algal Res.* **19**, 342–347 (2016). <https://doi.org/10.1016/j.algal.2016.02.008>
- Michalak, I., Chojnacka, K., Dobrzański, Z., Górecki, H., Zielińska, A., Korczyński, M., Opaliński, S.: Effect of macroalgae enriched with microelements on egg quality parameters and mineral content of eggs, eggshell, blood, feathers and droppings. *J. Anim. Physiol. Anim. Nutr. (Berl)* **95**, 374–387 (2011). <https://doi.org/10.1111/j.1439-0396.2010.01065.x>
- Saeid, A., Chojnacka, K., Korczyński, M., Korniewicz, D., Dobrzański, Z.: Biomass of *Spirulina maxima* enriched by biosorption process as a new feed supplement for swine. *J. Appl. Phycol.* **25**, 667–675 (2013). <https://doi.org/10.1007/s10811-012-9901-6>
- European Parliament and Council: Regulation (EC) No 767/2009 of the European Parliament and of the Council of 13 July 2009 on the placing on the market and use of feed. *Off. J. Eur. Union.* L 229/1–28 (2009)
- Kraujalienė, V., Pukalskas, A., Venskutonis, P.R.: Biorefining of goldenrod (*Solidago virgaurea* L.) leaves by supercritical fluid and pressurized liquid extraction and evaluation of antioxidant properties and main phytochemicals in the fractions and plant material. *J. Funct. Foods* **37**, 200–208 (2017). <https://doi.org/10.1016/j.jff.2017.07.049>
- Gao, D.W., Hu, Q., Pan, H., Jiang, J., Wang, P.: High-capacity adsorption of aniline using surface modification of lignocellulose-biomass jute fibers. *Bioresour. Technol.* **193**, 507–512 (2015). <https://doi.org/10.1016/j.biortech.2015.06.138>
- Sarada, B., Krishna Prasad, M., Kishore Kumar, K., Murthy, C.V.R.: Biosorption of Cd<sup>2+</sup> by green plant biomass, *Araucaria heterophylla*: characterization, kinetic, isotherm and thermodynamic studies. *Appl. Water Sci.* **7**, 3483–3496 (2017). <https://doi.org/10.1007/s13201-017-0618-1>
- Meseguer, V.F., Ortuño, J.F., Aguilar, M.I., Pinzón-Bedoya, M.L., Lloréns, M., Sáez, J., Pérez-Marín, A.B.: Biosorption of cadmium (II) from aqueous solutions by natural and modified non-living leaves of *Posidonia oceanica*. *Environ. Sci. Pollut. Res.* **23**, 24032–24046 (2016). <https://doi.org/10.1007/s11356-016-7625-x>
- Zhao, X., Zhu, H., Chen, J., Ao, Q.: FTIR, XRD and SEM analysis of ginger powders with different size. *J. Food Process. Preserv.* **39**, 2017–2026 (2015). <https://doi.org/10.1111/jfpp.12442>
- Wu, Y., Zhang, S., Guo, X., Huang, H.: Adsorption of chromium(III) on lignin. *Bioresour. Technol.* **99**, 7709–7715 (2008). <https://doi.org/10.1016/j.biortech.2008.01.069>

15. Jasicka-Misiak, I., Makowicz, E., Stanek, N.: Chromatographic fingerprint, antioxidant activity, and colour characteristic of polish goldenrod (*Solidago virgaurea* L.) honey and flower. *Eur. Food Res. Technol.* **244**, 1169–1184 (2018). <https://doi.org/10.1007/s00217-018-3034-3>
16. Izydorczyk, G., Skrzypczak, D., Kocek, D., Mironiuk, M., Witek-Krowiak, A., Moustakas, K., Chojnacka, K.: Valorization of bio-based post-extraction residues of goldenrod and alfalfa as energy pellets. *Energy* (2020). <https://doi.org/10.1016/j.energy.2020.116898>
17. Sahin, K., Onderci, M., Sahin, N., Aydin, S.: Effects of dietary chromium picolinate and ascorbic acid supplementation on egg production, egg quality and some serum metabolites of laying hens reared under a low ambient temperature (6°C). *Arch. Anim. Nutr.* **56**, 41–49 (2002). <https://doi.org/10.1080/00039420214174>
18. Sahin, N., Hayirli, A., Orhan, C., Tuzcu, M., Komorowski, J.R., Sahin, K.: Effects of the supplemental chromium form on performance and metabolic profile in laying hens exposed to heat stress. *Poult. Sci.* **97**, 1298–1305 (2018). <https://doi.org/10.3382/ps/pex435>
19. Onderci, M., Sahin, N., Sahin, K., Kilic, N.: Antioxidant properties of chromium and zinc: in vivo effects on digestibility, lipid peroxidation, antioxidant vitamins, and some minerals under a low ambient temperature. *Biol. Trace Elem. Res.* **92**, 139–150 (2003). <https://doi.org/10.1385/BTER:92:2:139>
20. Zhang, Y.N., Zhang, H.J., Wang, J., Yue, H.Y., Qi, X.L., Wu, S.G., Qi, G.H.: Effect of dietary supplementation of organic or inorganic zinc on carbonic anhydrase activity in eggshell formation and quality of aged laying hens. *Poult. Sci.* **96**, 2176–2183 (2017). <https://doi.org/10.3382/ps/pew490>
21. Tiecher, T.L., Ceretta, C.A., Ferreira, P.A.A., Lourenzi, C.R., Tiecher, T., Giroto, E., Nicoloso, F.T., Soriani, H.H., De Conti, L., Mimmo, T., Cesco, S., Brunetto, G.: The potential of *Zea mays* L. in remediating copper and zinc contaminated soils for grapevine production. *Geoderma* **262**, 52–61 (2016). <https://doi.org/10.1016/j.geoderma.2015.08.015>
22. Ibiang, Y.B., Mitsumoto, H., Sakamoto, K.: Bradyrhizobia and arbuscular mycorrhizal fungi modulate manganese, iron, phosphorus, and polyphenols in soybean (*Glycine max* (L.) Merr.) under excess zinc. *Environ. Exp. Bot.* **137**, 1–13 (2017). <https://doi.org/10.1016/j.envexpbot.2017.01.011>
23. Shahid, M., Shamsad, S., Rafiq, M., Khalid, S., Bibi, I., Niazi, N.K., Dumat, C., Rashid, M.I.: Chromium speciation, bioavailability, uptake, toxicity and detoxification in soil-plant system: a review. *Chemosphere* **178**, 513–533 (2017). <https://doi.org/10.1016/j.chemosphere.2017.03.074>
24. Drelinkiewicz, A., Knapik, A., Waksmundzka-Góra, A., Bukowska, A., Bukowski, W., Noworól, J.: Functional gel-type resin based palladium catalysts: the role of polymer properties in the hydrogenation of the C{double bond, long}C bond of maleic and fumaric acids, the isomers of dicarboxylic acids. *React. Funct. Polym.* **68**, 1059–1071 (2008). <https://doi.org/10.1016/j.reactfunctpolym.2008.02.008>
25. Armbruster, M.H., Austin, J.B.: The adsorption of gases on plane surfaces of mica. *J. Am. Chem. Soc.* **60**, 467–475 (1918). <https://doi.org/10.1021/ja01269a066>
26. Freundlich, H.: Über die adsorption in Lösungen. *Zeitschrift-Physik* **LXII**, 385–471 (1957)
27. Malhotra, M., Suresh, S., Garg, A.: Tea waste derived activated carbon for the adsorption of sodium diclofenac from wastewater: adsorbent characteristics, adsorption isotherms, kinetics, and thermodynamics. *Environ. Sci. Pollut. Res.* **25**, 32210–32220 (2018). <https://doi.org/10.1007/s11356-018-3148-y>
28. Jeppu, G.P., Clement, T.P.: A modified Langmuir-Freundlich isotherm model for simulating pH-dependent adsorption effects. *J. Contam. Hydrol.* **129–130**, 46–53 (2012). <https://doi.org/10.1016/j.jconhyd.2011.12.001>
29. Upton, G.J.G.: Fisher's exact test. *R. Stat. Soc.* **155**, 395–402 (1992)
30. ISTA: International rules for seed testing: edition 2016 (2016)
31. Jyske, T., Hölltä, T.: Comparison of phloem and xylem hydraulic architecture in *Picea abies* stems. *New Phytol.* **205**, 102–115 (2015). <https://doi.org/10.1111/nph.12973>
32. Thomson, C.A., Chesney, D.J.: Supercritical carbon dioxide extraction of 2, 4-dichlorophenol from food crop tissues. *Anal. Chem.* **64**, 848–853 (1992). <https://doi.org/10.1021/ac00032a006>
33. Ziyath, A.M., Mahbub, P., Goonetilleke, A., Adebajo, M.O., Kokot, S., Oloyede, A.: Influence of physical and chemical parameters on the treatment of heavy metals in polluted stormwater using zeolite: a review. *J. Water Resour. Prot.* **03**, 758–767 (2011). <https://doi.org/10.4236/jwarp.2011.310086>
34. Vanholme, R., Demedts, B., Morreel, K., Ralph, J., Boerjan, W.: Lignin biosynthesis and structure. *Plant Physiol.* **153**, 895–905 (2010). <https://doi.org/10.1104/pp.110.155119>
35. Yruela, I.: Copper in plants. *Braz. J. Plant Physiol.* **17**, 145–156 (2005). <https://doi.org/10.1590/s1677-04202005000100012>
36. Faried, A., Zareh, M., Nafady, N., Mohamed, M.: Green synthesis of silver nanoparticles from capitula extract of some *Launaea* (Asteraceae) with notes on their taxonomic significance. *Egypt. J. Bot.* (2018). <https://doi.org/10.21608/ejbo.2018.1375.1111>
37. Nasef, S., ElNesr, E., Hafez, F., Badawy, N., Slim, S.: Gamma irradiation induced preparation of gum arabic/ poly (vinyl alcohol) copolymer hydrogels for removal of heavy metal ions from wastewater. *Arab. J. Nucl. Sci. Appl.* (2019). <https://doi.org/10.21608/ajnsa.2019.15587.1246>
38. Yah, W.O., Takahara, A., Lvov, Y.M.: Selective modification of halloysite lumen with octadecylphosphonic acid: new inorganic tubular micelle. *J. Am. Chem. Soc.* **134**, 1853–1859 (2012). <https://doi.org/10.1021/ja210258y>
39. Hoekman, S.K., Broch, A., Robbins, C.: Hydrothermal carbonization (HTC) of lignocellulosic biomass. *Energy Fuels* **25**, 1802–1810 (2011). <https://doi.org/10.1021/ef101745n>
40. Hussain, N., Abbasi, T., Abbasi, S.A.: Vermicomposting transforms allelopathic parthenium into a benign organic fertilizer. *J. Environ. Manag.* **180**, 180–189 (2016). <https://doi.org/10.1016/j.jenvman.2016.05.013>
41. Adel, A.M., Abd El-Wahab, Z.H., Ibrahim, A.A., Al-Shemy, M.T.: Characterization of microcrystalline cellulose prepared from lignocellulosic materials. Part II: physicochemical properties. *Carbohydr. Polym.* **83**, 676–687 (2011). <https://doi.org/10.1016/j.carbpol.2010.08.039>
42. Islam, N.U., Jalil, K., Shahid, M., Rauf, A., Muhammad, N., Khan, A., Shah, M.R., Khan, M.A.: Green synthesis and biological activities of gold nanoparticles functionalized with *Salix alba*. *Arab. J. Chem.* **12**, 2914–2925 (2019). <https://doi.org/10.1016/j.arabjch.2015.06.025>
43. Pérez Marín, A.B., Aguilar, M.I., Meseguer, V.F., Ortuño, J.F., Sáez, J., Lloréns, M.: Biosorption of chromium (III) by orange (*Citrus cinensis*) waste: batch and continuous studies. *Chem. Eng. J.* **155**, 199–206 (2009). <https://doi.org/10.1016/j.cej.2009.07.034>
44. Li, M., Wang, L.J., Li, D., Cheng, Y.L., Adhikari, B.: Preparation and characterization of cellulose nanofibers from de-pectinated sugar beet pulp. *Carbohydr. Polym.* **102**, 136–143 (2014). <https://doi.org/10.1016/j.carbpol.2013.11.021>
45. Hu, Z.H., Omer, A.M., Ouyang, X.K., Yu, D.: Fabrication of carboxylated cellulose nanocrystal/sodium alginate hydrogel beads for adsorption of Pb(II) from aqueous solution. *Int. J. Biol. Macromol.* **108**, 149–157 (2018). <https://doi.org/10.1016/j.ijbiomac.2017.11.171>
46. Kazemi, M., Khodaiyan, F., Labbafi, M., Saeid Hosseini, S., Hojjati, M.: Pistachio green hull pectin: optimization of



- microwave-assisted extraction and evaluation of its physico-chemical, structural and functional properties. *Food Chem.* **271**, 663–672 (2019). <https://doi.org/10.1016/j.foodchem.2018.07.212>
47. Reynel-Avila, H.E., Mendoza-Castillo, D.I., Olumide, A.A., Bonilla-Petriciolet, A.: A survey of multi-component sorption models for the competitive removal of heavy metal ions using bush mango and flamboyant biomasses. *J. Mol. Liq.* **224**, 1041–1054 (2016). <https://doi.org/10.1016/j.molliq.2016.10.061>
  48. De Ruiter, J.: *Carboxylic Acid Structure and Chemistry* : Part 2. Springer, New York (2005)
  49. Repo, E., Petrus, R., Sillanpää, M., Warchoń, J.K.: Equilibrium studies on the adsorption of Co(II) and Ni(II) by modified silica gels: one-component and binary systems. *Chem. Eng. J.* **172**, 376–385 (2011). <https://doi.org/10.1016/j.cej.2011.06.019>
  50. Ma, W., Gu, Y., Lu, J., Yuan, L., Zhao, R.: Effects of chromium propionate on egg production, egg quality, plasma biochemical parameters, and egg chromium deposition in late-phase laying hens. *Biol. Trace Elem. Res.* **157**, 113–119 (2014). <https://doi.org/10.1007/s12011-013-9875-5>
  51. Króliczewska, B., Zawadzki, W., Skiba, T., Miąta, D.: Effects of chromium supplementation on chicken broiler growth and carcass. *Acta Vet. Brno* **74**, 543–549 (2005)
  52. EU Commission: List of authorised additives in feedingstuffs; published in application of Article 9t of Council Directive 70/524/EEC concerning additives in feedingstuffs. *Off. J. Eur. Union* **C50**, 1–144 (2004)
  53. Tuhy, L., Samoraj, M., Chojnacka, K.: Evaluation of nutrients bioavailability from fertilizers in in vivo tests. *Interdiscip. J. Eng. Sci.* **1**, 10–13 (2013)
  54. Sharififar, A., Nazari, M., Asghari, H.R.: Effect of ultrasonic waves on seed germination of *Atriplex lentiformis*, *Cuminum cyminum*, and *Zygophyllum eurypterum*. *J. Appl. Res. Med. Aromat. Plants.* **2**, 102–104 (2015). <https://doi.org/10.1016/j.jar-map.2015.05.003>
  55. Deng, B., Tian, S., Li, S., Guo, M., Liu, H., Li, Y., Wang, Q., Zhao, X.: A simple, rapid and efficient method for essential element supplementation based on seed germination. *Food Chem.* **325**, 126827 (2020). <https://doi.org/10.1016/j.foodchem.2020.126827>
  56. Samreen, T., Shah, H.U., Ullah, S., Javid, M.: Zinc effect on growth rate, chlorophyll, protein and mineral contents of hydroponically grown mungbeans plant (*Vigna radiata*). *Arab. J. Chem.* **10**, S1802–S1807 (2017). <https://doi.org/10.1016/j.arabjc.2013.07.005>
  57. Adamo, P., Iavazzo, P., Albanese, S., Agrelli, D., De Vivo, B., Lima, A.: Bioavailability and soil-to-plant transfer factors as indicators of potentially toxic element contamination in agricultural soils. *Sci. Total Environ.* **500–501**, 11–22 (2014). <https://doi.org/10.1016/j.scitotenv.2014.08.085>
  58. Izydorczyk, G., Sienkiewicz-Cholewa, U., Baśladyńska, S., Kocek, D., Mironiuk, M., Chojnacka, K.: New environmentally friendly bio-based micronutrient fertilizer by biosorption: from laboratory studies to the field. *Sci. Total Environ.* **710**, 136061 (2020). <https://doi.org/10.1016/j.scitotenv.2019.136061>
  59. Dean, J.R.: *Bioavailability, Bioaccessibility and Mobility of Environmental Contaminants*, p. 32. Wiley, Hoboken (2007)
  60. Zou, T., Xu, N., Hu, G., Pang, J., Xu, H.: Biofortification of soybean sprouts with zinc and bioaccessibility of zinc in the sprouts. *J. Sci. Food Agric.* **94**, 3053–3060 (2014). <https://doi.org/10.1002/jsfa.6658>

**Publisher's Note** Springer Nature remains neutral with regard to jurisdictional claims in published maps and institutional affiliations.